Neutral particle drag on parallel flow shear driven instability

M. Sasaki*[1, 2], T. Kobayashi[3], S. Inagaki[1, 2], N. Kasuya[1, 2], and Y. Kosuga[1, 2]

[1]Research Institute for Applied Mechanics, Kyushu University, Kasuga 816-8580, Japan
[2]Research Center for Plasma Turbulence, Kyushu University, Kasuga 816-8580, Japan
[3]National Institute for Fusion Science, Toki 509-5292, Japan

Abstract

Neutral drag effect on the parallel velocity gradient driven instability (PVG) in the presence of density inhomogeneity is theoretically investigated. The dispersion relation of PVG mode with the effect of density gradient and neutral particle drag is derived, and its solution is analytically obtained. The neutral particle drag gives rise to the phase shift between parallel flow and electrostatic potential fluctuations, and modifies the parallel compression. As a result, the stability of the PVG mode changes. It is found that the neutral particle drag does not only reduces but also enhances the instability. Especially, near the marginal condition, the neutral particle effect suppresses the density gradient effect, and the parameter region where the PVG mode is linearly unstable significantly expands.

1 Introduction

In magnetically confined plasmas, plasma flows parallel to the magnetic field [1, 2, 3] play important roles of controlling the MHD instability and of suppression of turbulence [4]. The shear of the parallel flow can be a free energy source for the instability, which is called D'Angelo mode or parallel velocity gradient (PVG) mode or Kelvin-Helmholtz (KH) instability[5]. (In this study, we use PVG mode to describe the parallel flow shear instability, and we use perpendicular KH instability for that due to the perpendicular flow inhomogeneity [6, 7].) The PVG mode has been identified in a basic experiment [8]. The PVG mode is important for the cases of NBI plasmas [9], internal transport barrier [10, 11], and scrape off layer (SoL) [12]. PVG mode has been found to drive the inward particle flux theoretically and experimentally [13, 14, 15]. Recently, it has been pointed out that PVG mode in the H-mode plasmas can be precursor of the type-III ELM [16, 17].

*corresponding author: sasaki@riam.kyushu-u.ac.jp

In this way, PVG mode has been an important topic in the study of magnetic confined plasmas.

The parallel flow is often strong in a low temperature plasma, such as in the SoL and in basic experiments [8, 18, 19]. In such plasmas, neutral particles exist and drag the flow, which should be taken into account. In the series of studies on PVG mode in confined plasmas, the neutral particle effect has not been considered [9, 10, 11, 12, 13]. For the space plasmas, the PVG mode with the effect of neutral particles has been analyzed without considering the density inhomogeneity. Density inhomogeneity is important for the confinement plasmas, which suppresses the PVG mode linearly and nonlinearly [12, 13, 20]. Thus, it is important to study the PVG mode stability with considering the neutral particle effect and the density inhomogeneity. In this study, we investigate the neutral particle effect on the PVG mode stability in the presence of the density inhomogeneity. The rest of the paper is organized as follows. In section 2, the model equations are introduced, and the dispersion relation of the PVG mode is derived. The characteristics of its solution of the dispersion relation are discussed in section 3. The summary is given in section 4.

2 Model

In this section, the situation we consider is described, the reduced fluid model equations are introduced. Then, the dispersion relation of the PVG mode with the effect of the neutral particle is derived with the assumption of the Boltzmann relation between the density and the potential fluctuations. With this assumption, the drift wave becomes linearly stable, and we can avoid the hybrid branch of the PVG and the drift wave [21].

We consider inhomogeneous magnetized plasmas, where the magnetic field direction is chosen to be z-direction, and the density and the parallel flow have gradients in x-direction. This situation is similar to that of the basic plasma experiment in a linear device, where the drift wave and the PVG mode have been observed [8, 14, 15, 22, 23]. In such a situation, Hasegawa-Wakatani model coupling with the parallel flow [20, 21] can be used, which is derived from the electrostatic two fluid equation (the details of the model is described in Appendix.A). The model equations are given as follows

$$\partial_t N + \left[\phi, N\right] = -V\nabla_\parallel N - D\nabla_\parallel^2 (\phi - N) - \nabla_\parallel V, \tag{1a}$$

$$\partial_t \nabla_\perp^2 \phi + \left[\phi, \nabla_\perp^2 \phi\right] = -V\nabla_\parallel \nabla_\perp^2 \phi - D\nabla_\parallel^2 (\phi - N) - \nu\nabla_\perp^2 \phi, \tag{1b}$$

$$\partial_t V + \left[\phi, V\right] = -V\nabla_\parallel V - \nabla_\parallel N - \nu V. \tag{1c}$$

Here, N, ϕ, V are the normalized electron density, electrostatic potential and ion parallel flow, which are normalized by the stationary density, electron temperature and the sound speed, respectively. The space and time are normalized by the ion gyro-radius calculated by the sound speed and the ion gyro-frequency, respectively. The convective derivative, $[\phi, \cdots]$, is expressed by using the Poisson bracket. The parallel diffusivity is denoted by D and the ion-neutral collision frequency are expressed by ν. The neutral particle effect is introduced by the drag forces on flows due to the ion-neutral collision (the last terms

of Eq. (1b) and Eq.(1c) in the RHS), which we focus on as the dominant neutral particle effect. Although these terms have been considered in numerical turbulence simulations [20, 21, 7] and a theoretical study [24], the stability analysis of the PVG mode that focuses on the effect of the neutral drag terms has not been performed, which is the central topic of this paper.

The linear dispersion relation of the PVG mode is derived by neglecting the nonlinear terms. First, we express the physical quantity as $X = \langle X \rangle + \tilde{X}$, where $X = \{N, \phi, V\}$, and $\langle X \rangle$ is the stationary part and $\tilde{X}$ is the fluctuating part. The spatial derivative in x for the stationary density and parallel flow, $\partial_x \langle N \rangle$ and $\partial_x \langle V \rangle$, are finite. The stationary component of the potential, whose spatial derivative drives the perpendicular flow through $E \times B$ drift, is assumed to be constant in space in order to exclude the perpendicular KH instability [6, 7] and to focus on the PVG mode. The fluctuating part is decomposed into Fourier modes as $\tilde{X} = X_k \exp(-i\omega t + i\boldsymbol{k} \cdot \boldsymbol{x})$. Using the Fourier modes, the convective derivative terms for the density and the parallel flow are calculated as

$$[\phi, N]_k = i\omega_n \phi_k, \tag{2a}$$
$$[\phi, V]_k = -i\omega_V \phi_k, \tag{2b}$$

where $\omega_n = -k_y \partial_x \langle N \rangle$ and $\omega_V = k_y \partial_x \langle V \rangle$ indicate the inhomogeneity. The linearized response of the parallel flow perturbation is obtained as

$$V_k = -\left(1 + i\frac{\nu}{\Omega}\right)^{-1} \left[\frac{\omega_V}{\Omega}\phi_k - \frac{k_\parallel}{\Omega} N_k\right], \tag{3}$$

where Ω is the frequency with the Doppler shift, defined by $\Omega = \omega - k_\parallel \langle V \rangle$. Due to the neutral particle drag, the phase shift between the parallel flow and the potential and density perturbations becomes finite. The parallel flow perturbation contributes to the parallel compression through the last term in Eq. (1a) of RHS, so that the phase shift due to the neutral particle drag modifies the property of the parallel compression and as a consequence the stability significantly changes. Combining the Eqs. (1a), (1b) and Eq. (3) to eliminate the parallel diffusion terms, we obtain

$$\left(\Omega - \frac{k_\parallel^2}{\Omega + i\nu}\right) N_k + \left(-\omega_n + k_\perp^2 \Omega + i\nu k_\perp^2 + \frac{k_\parallel \omega_V}{\Omega + i\nu}\right) \phi_k = 0. \tag{4}$$

The relation between the density and potential perturbations is obtained from Eq. (1b) as

$$N_k = \left[1 - i\frac{k_\perp^2 (\Omega + i\nu)}{D k_\parallel^2}\right] \phi_k. \tag{5}$$

The second term in the square bracket causes the phase shift between the density and potential. Conventionally, $Dk_\parallel^2 \gg 1$ is assumed, and the phase shift is treated as a smallness parameter [21]. If one considers the resistive drift wave instability, the finite phase difference is necessary to realize the instability. For the PVG mode, the phase shift

between the density and potential is not necessary for the destabilization [13]. Therefore, in this study, we consider a limit, $Dk_\parallel^2 \gg 1$, and $N_k = \phi_k$ is obtained, which is the Boltzmann relation. Using the Boltzmann relation, the dispersion relation $\Delta = 0$ is obtained as

$$\Delta = \Omega - \omega_D + i\nu\alpha - \frac{k_\parallel^2 - k_\parallel \omega_V}{(\Omega + i\nu)(1 + k_\perp^2)} = 0, \tag{6}$$

where $\omega_D = \omega_n(1+k_\perp^2)^{-1}$ and $\alpha = k_\perp^2(1+k_\perp^2)^{-1}$. The fourth term stems from the coupling with the parallel flow. If one neglects the coupling with the parallel flow (this corresponds to the limit, $k_\parallel \to 0$), the drift wave branch is obtained as

$$\Omega = \omega_D - i\alpha\nu. \tag{7}$$

It is noted that the phase difference between the density and potential is neglected, and thus only damping due to the neutral particle drag appears. On the other hand, when one ignores the inhomogeneities of the density and parallel flow, $\omega_n \to 0$ and $\omega_V \to 0$. Then, the ion sound wave branch is obtained as

$$\Omega = \frac{\pm k_\parallel}{\sqrt{1 + k_\perp^2}} - i\nu\frac{\alpha + 1}{2}. \tag{8}$$

As seen above, the neutral particle drag works as the damping for the ion sound wave, as well (where the higher order of ν is not considered here). In the next section, we discuss the PVG branch obtained from Eq. (6), and describe the neutral particle drag effect on the PVG mode.

3 Stability of PVG including neutral particle drag

In this section, we describe the properties of the solution of the dispersion relation Eq. (6), and show that, due to the neutral particle drag effect, the parameter regime where the PVG mode is linearly unstable significantly expands.

First, we remind the PVG stability without the neutral particle drag. In this limit, $\nu \to 0$, and the PVG mode branch is obtained as

$$\Omega = \frac{1}{2}\left[\omega_D + \sqrt{\omega_D^2 + 4\frac{k_\parallel^2 - k_\parallel\omega_V}{1 + k_\perp^2}}\right]. \tag{9}$$

The linear instability arises when the term in the square root becomes negative. This condition is expressed as [12, 13]

$$k_\parallel\omega_V - k_\parallel^2 > \frac{1}{4}\left(1 + k_\perp^2\right)\omega_D^2. \tag{10}$$

Here, the sign of the LHS terms, $k_\parallel\omega_V - k_\parallel^2$, is the same as that of the parallel compressional term $-\nabla_\parallel V$. In order for the PVG to be unstable, the negative compression is necessary,

and the density inhomogeneity gives the critical threshold for the instability. From the instability condition, Eq. (10), one sees that the density gradient, which corresponds to ω_D, increases the threshold for the PVG mode to be unstable, and thus the PVG mode is rarely driven in the presence of the steep density profile. From Eq. (9), the the most unstable parallel wavenumber, which maximizes the growth rate, is found to be $k_\parallel = \omega_V/2$.

Next, we describe the neutral particle drag effect. Equation (6) is numerically solved to show how the topology of the solution curves in the complex plane changes due to the neutral particles, which is shown in Fig. 1, where the following parameters are used in the calculations, $k_\perp = 0.3, k_\parallel = 0.05$ and $\omega_V = 0.1$. In order to clarify the neutral particle effect, we show the following four cases in Fig. 1: one is with $\omega_n = 0.09$, which satisfies the marginal condition without the neutral particle Eq. (10) for (a)$\nu = 0$ and (b)$\nu = 0.02$, and the other is with $\omega_n = 0.12$, which does not satisfy Eq. (10) for (c)$\nu = 0$ and (d)$\nu = 0.02$. The black and red lines correspond to the lines which satisfy $\mathrm{Re}\Delta = 0$ and $\mathrm{Im}\Delta = 0$, respectively, so that the solutions are the points of the intersection of them. For the case of Fig. 1(a), $(\mathrm{Re}\omega, \mathrm{Im}\omega) = (0.041, 0.024)$ is the unstable PVG branch, and $(0.053, 0.019)$ is the solution for Fig. 1(b). The growth rate, $\mathrm{Im}\omega$, becomes small due to the neutral particle drag in this case. On the other hand, in the case when the density gradient is large and Eq. (10) is not satisfied, the solution $(\mathrm{Re}\omega, \mathrm{Im}\omega) = (0.083, 0.0)$ without the neural particle effect, Fig. 1(c), is modified to be $(0.087, 0.0066)$ due to the neutral particle drag as in Fig. 1(d). The neutral particle drag increases the growth rate. As seen, the topology of the solution curves change due to the neutral particles; the curves which satisfy $\mathrm{Im}\Delta = 0$ are symmetry with respect to the sign of $\mathrm{Im}\Omega$ without the neutral particles, and change to be asymmetry with finite ν. The curves which satisfy $\mathrm{Re}\Delta = 0$ also becomes asymmetry to the sign of $\mathrm{Im}\Omega$ due to the neutral particles, and a closed curve appears in addition to a line which extends from up to down in the case of $\omega_n = 0.12$ (Eq. (10) is not satisfied). In this way, the neutral particle drag does not always reduces but also enhances the growth rate, depending on the parameters.

The analytical solution of the dispersion relation Eq. (6) can be expressed as

$$\Omega = \frac{1}{2}\left[\omega_D + \frac{1}{\sqrt{2}}\sqrt{D_r + \sqrt{D_r^2 + D_i^2}} + i\left\{ -(1+\alpha)\,\nu + \frac{1}{\sqrt{2}}\sqrt{-D_r + \sqrt{D_r^2 + D_i^2}}\right\}\right], \quad (11)$$

where D_r and D_i are defined as

$$D_r = \omega_D^2 + 4\frac{k_\parallel^2 - k_\parallel \omega_V}{1 + k_\perp^2} - \nu^2\,(\alpha - 1)^2\,, \quad (12a)$$

$$D_i = 2\,(1-\alpha)\,\omega_D \nu, \quad (12b)$$

respectively. This expression agrees with Eq. (9) in the limit of $\nu \to 0$. Without the neutral particle effect, the instability condition is $D_r < 0$, which agrees with Eq. (10), as well. The term D_i stems from the coupling with the neutral particle effect and the density inhomogeneity, which significantly affects the stability of the PVG mode. As seen in the imaginary part of Eq. (11), $D_r < 0$ is not required for PVG mode to be unstable

when D_i is finite. The instability condition is given as

$$\sqrt{D_r^2 + D_i^2} - D_r > 2\left(1+\alpha\right)^2 \nu^2, \tag{13}$$

which can reproduce Eq. (10) in the limit of $\nu \to 0$. Equation (13) can be rewritten as follows only when $D_r > 0$ (the conventional PVG mode is stable) and $\nu \neq 0$.

$$k_\parallel \omega_V - k_\parallel^2 > \frac{\alpha\left(1+k_\perp^2\right)}{\left(1+\alpha\right)^2}\omega_D^2 + \alpha\left(1+k_\perp^2\right)\nu^2. \tag{14}$$

Noted that this can not reproduce Eq. (10), because the devision by ν is performed and $D_r > 0$ is assumed. The first term in the RHS is the density inhomogeneity effect and the second term is the neutral particle effect. These two terms determine the threshold for the PVG instability. The coefficient of the density term, ω_D^2 (the first term in the RHS), is significantly reduced by the neutral particle effect, as $\alpha\left(1+k_\perp^2\right)\left(1+\alpha\right)^{-2} = k_\perp^2\left(1+k_\perp^2\right)^2\left(1+2k_\perp^2\right)^{-2}$. Here, the wavelength of the PVG is typically longer than the ion gyro-radius, $k_\perp < 1$. It is noted that this coefficient becomes $\left(1+k_\perp^2\right)/4$ without the neutral particle effect, which is much larger compared to that with the neutral particle effect. Thus, the neutral particle drag largely suppresses the critical vale for the instability. As seen in Eq. (14), the sign of the LHS term is the same as the parallel compression, and thus the negative compression is still necessary for the instability. Noted that the most unstable parallel wavenumber is $k_\parallel = \omega_V/2$, which is the same with the case without the neutral particle effect.

Figure 2 illustrates the dependence of the real frequency and the growth rate on the neutral particle drag, where one is the case when Eq. (10) is satisfied ((a) $\omega_n = 0.09$), and the other is not ((b) $\omega_n = 0.12$). The real frequencies for both cases gradually increase with the neutral particle drag. The growth rate in the case when Eq. (10) is satisfied constantly decreases with the neutral particle drag. In the case when Eq. (10) is not satisfied, the growth rate once increases and then decreases with the drag, so it has a peak around $\nu \sim 0.04$, and becomes stable when $\mathrm{Re}\omega \sim \nu$.

The instability diagram in the $\omega_n - \omega_V$ plane is shown in Fig. 3 in the case of $\nu = 0.02$, where the color corresponds to the growth rate of the PVG mode. The solid and dashed lines are the marginal conditions for $\nu = 0.02$ and $\nu = 0$, respectively. When both the density gradient and the parallel flow shear are not strong ($\omega_n < 0.1, \omega_V < 0.1$), the parallel flow shear which is necessary for the instability becomes large due to the neutral particle drag. Thus, in this region, the neutral particle effect works to suppress the instability. On the other hand, in the case of the strong density gradient ($\omega_n > 0.1$), the instability region expands significantly due to the neutral particle effect. Therefore, the PVG mode can be unstable even with the steep density profile when there are sufficient number of neutral particles. The neutral particle drag gives rise to the phase shift between the parallel flow and potential fluctuations, which modifies the parallel compression, and thus the stability of the PVG mode is greatly changed. In particular, near the marginal condition, the effect of the neutral particles becomes important, and the instability region greatly widens.

Next, we discuss the characteristics of the eigenfunction, which is useful for the experimental identification. The amplitude and phase relations between the parallel flow and potential fluctuation is given as follows by using Eq. (3) and the Boltzmann relation.

$$\frac{|V_k|}{|\phi_k|} = \frac{|\omega_V - k_\parallel|}{\sqrt{\Omega^2 + \nu^2}}, \tag{15a}$$

$$\tan\Psi = \frac{\mathrm{Im}\left[V_k \phi_k^*\right]}{\mathrm{Re}\left[V_k \phi_k^*\right]} = \frac{\nu k_\parallel}{\Omega \omega_V}, \tag{15b}$$

The amplitude of the parallel flow fluctuation normalized by the potential decreases with the neutral particle drag. Noted that the expression, Eq. (15a), is just for the identification of the PVG mode in experiments. The sign of the phase difference Ψ is determined by the combination of $k_\parallel$ and ω_V. The characteristics of the eigenfunction are drawn in Fig. 4, by using Eqs. (15a) and (15b) with the solution of the dispersion relation. The amplitude of the parallel flow fluctuation normalized by the potential is above unity without the neutral particle effect [25], but with the neutral particle effect it typically becomes $|V_k|/|\phi_k| \sim 0.5$. The phase difference increases with the neutral particle drag, where it is noted that the reason why the phase shift becomes zero at $\nu = 0$ is that we assume the Boltzmann relation.

Finally, we discuss the stability of the PVG mode in the basic experiments in linear magnetized plasmas. The plasma parameters are chosen to be typical values as $L_n = 3$[cm], $L_V = 1$[cm] and $\rho_s = 5$[mm], where L_n and L_V are the scale length of the density and the parallel flow, respectively [14, 15, 26, 27]. When the Mach number M is $M = 0.5$ and $k_y = 0.5$, ω_n and ω_V are estimated as $\omega_n = 0.17$ and $\omega_V = 0.13$. These values are similar to those of PANTA device [14, 15]. The ion-neutral collision frequency is assumed to be $\nu = 0.02$ [28, 29]. This situation corresponds to the case when the instability condition without the neutral drag effect, Eq. (10), is not satisfied, but that with the neutral effect, Eq. (14), is satisfied (it is in the region between solid and dashed lines in Fig. 3). The proposed mechanism of the neutral effect can be important. Recently, neutral particle control experiment has been performed without changing the plasma profiles by using the gas-puffing, and the increase of the fluctuation with the neutral particles is observed [30]. The validation of the present mechanism is desired in such kind of experiments. In addition, in the SoL regions of toroidal plasmas, the plasma parameters are similar to those of the linear devices. Thus, the neutral drag effect proposed in this paper could be significant to drive the PVG mode in such cases.

It is noted that, in this paper, we simplify the model to focus on the roles of the neutral particles on the stability of the PVG mode. In the basic experiments and the SoL region of toroidal plasmas, the sheath effect exists, which affects the divergence of the parallel current, so that the turbulence properties could be modified by the sheath effect [31, 32]. The stability of the PVG mode in the presence of the sheath effect is beyond the scope of this study, which should be the future work. Moreover, in this study, we neglect the perpendicular KH instability, which is often important in the basic experiments [7, 31]. The nonlinear interaction between the PVG mode and the perpendicular KH would be interesting.

4 Summary

Neutral drag effect on the PVG mode in the presence of density inhomogeneity is studied, and the dispersion relation is derived. The analytical expression of its solution is derived and its characteristics are discussed. The neutral particle drag causes the phase shift between the parallel flow and the electrostatic potential fluctuations, and modifies the parallel compression. As a result, the stability of the PVG mode changes. It is found that the neutral particle drag does not only reduces but also enhances the instability. Especially, near the marginal condition, the neutral particle drag effect suppresses the density gradient effect and the parameter region where the PVG mode is linearly unstable significantly expands. A sufficient number of neutral particles exists in a low temperature region of plasmas, such as basic plasma experiments, and edge regions of toroidal plasmas (including SoLs). In such cases, the parallel flow is often strong, so that the PVG mode could dominate the transport and the system evolutions.

Acknowledgement

The authors acknowledge stimulating discussion with Prof. K. Itoh and the late Prof. S. -I. Itoh. The paper is dedicated to the late Prof. S. -I. Itoh. This work was partly supported by a grant-in-aid for scientific research of JSPS KAKENHI Grant Number (JP16K18335, JP17H06089, JP16H02442, JP15H02155, JP18K03578), the collaboration programs of NIFS (NIFS19KNST151, NIFS20KNST179), Asada Science Foundation, Progress 100 of Kyushu University (NB80645028), and the RIAM of Kyushu University.

Data availability

The data that support the findings of this study are available from the corresponding author upon reasonable request.

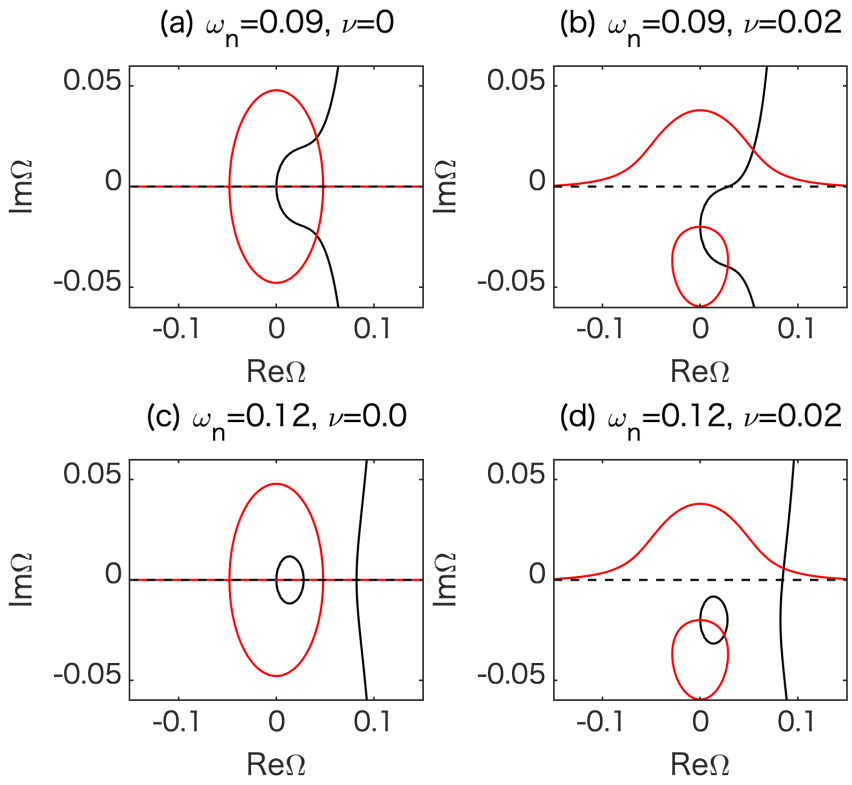

Fig. 1: Solutions of the dispersion relation Eq. (6) in complex plane in cases of (a) $\omega_n = 0.09, \nu = 0.0$, (b) $\omega_n = 0.09, \nu = 0.02$, (c) $\omega_n = 0.12, \nu = 0.0$, and (d) $\omega_n = 0.12, \nu = 0.02$. Here, the black and red lines indicate the lines which satisfy $\mathrm{Re}\Delta = 0$ and $\mathrm{Im}\Delta = 0$, respectively, and thus the solutions correspond to the intersections of the black and red lines.

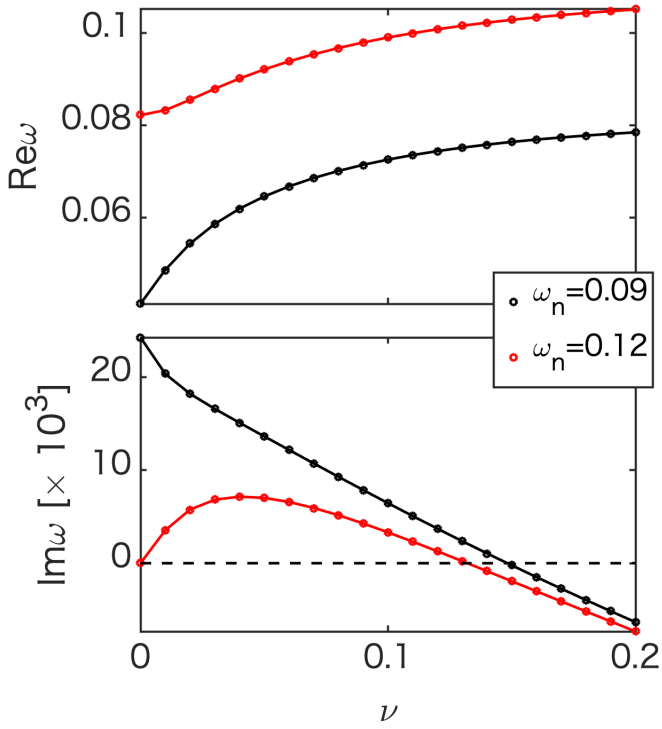

Fig. 2: Dependence of neutral particle drag on (a) the eigenfrequency and (b) the growth rate of the PVG mode. The numerical solutions of Eq. (6) in the cases of $\omega_n = 0.09$ and 0.12 are shown in black and red lines, respectively.

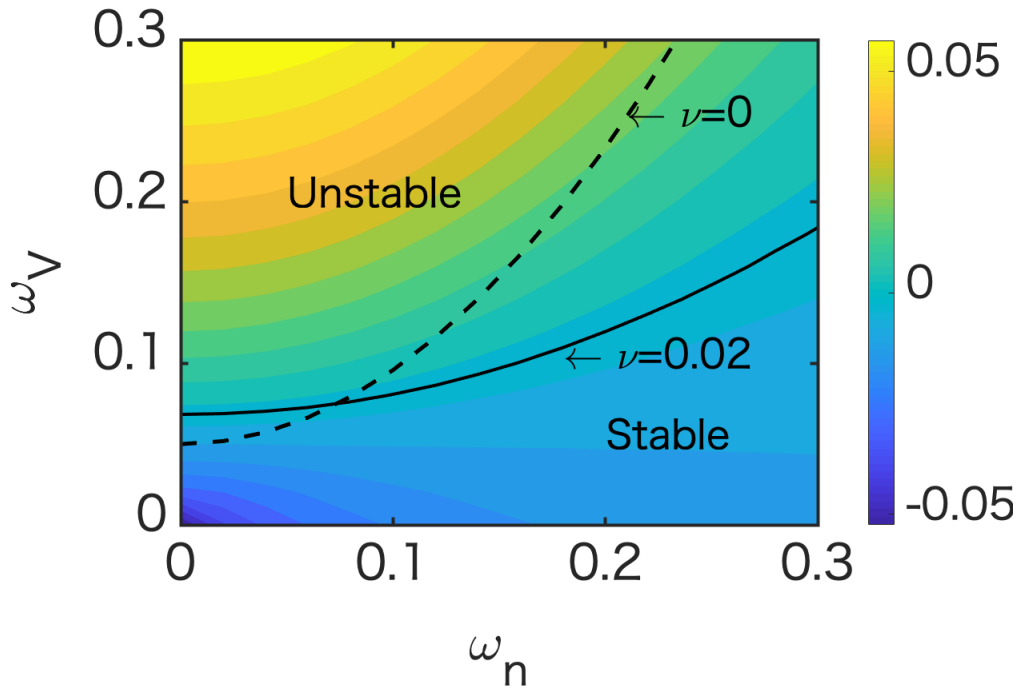

Fig. 3: Contour of growth rate of the PVG mode with $\nu = 0.02$. The solid and dashed lines are the marginal conditions for the PVG mode in the cases of $\nu = 0.02$ and $\nu = 0$, respectively, which correspond to Eq. (14), and Eq. (10). The region where the PVG mode becomes linearly unstable significantly expands.

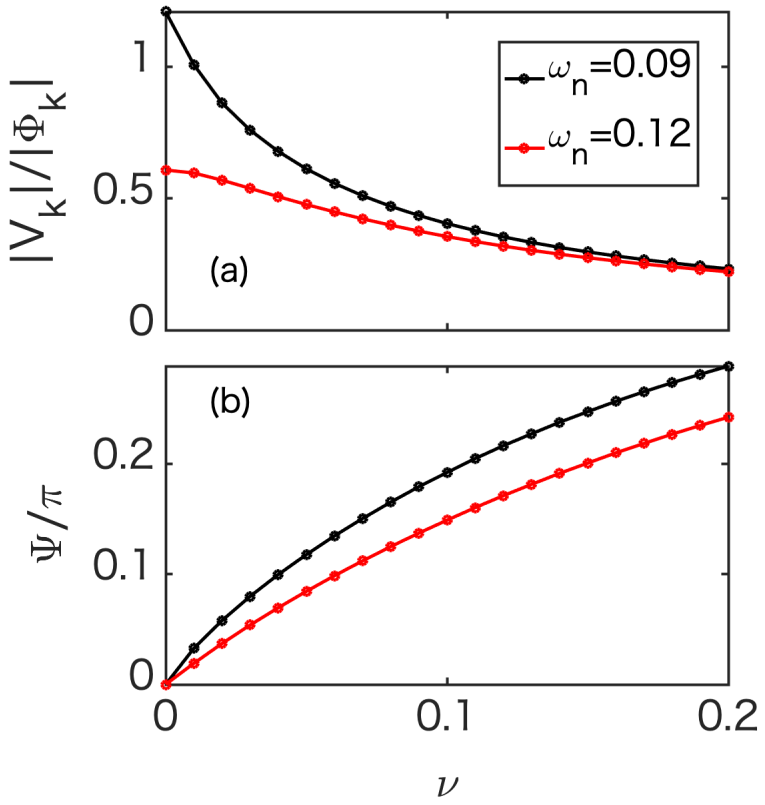

Fig. 4: Dependence of eigenfunction for the parallel velocity fluctuation on the neutral particle drag in the cases of $\omega_n = 0.09$ and 0.12 with $\nu = 0.02$.

A Brief summary of model equation

In order to describe turbulence, whose frequency is much lower than the ion gyro-frequency, we consider the electrostatic two fluid equations given as

$$\partial_t n_e + \nabla \cdot (n_e \boldsymbol{v}_e) = 0, \tag{A.1 a}$$
$$m_e n_e (\partial_t \boldsymbol{v}_e + \boldsymbol{v}_e \cdot \nabla \boldsymbol{v}_e) = -\nabla p_e - e n_e (-\nabla\phi + \boldsymbol{v}_e \times \boldsymbol{B}) - m_e n_e \nu_{ei} (\boldsymbol{v}_e - \boldsymbol{v}_i), \tag{A.1 b}$$
$$m_i n_i (\partial_t \boldsymbol{v}_i + \boldsymbol{v}_i \cdot \nabla \boldsymbol{v}_i) = -\nabla p_i + e n_i (-\nabla\phi + \boldsymbol{v}_i \times \boldsymbol{B}) - m_i n_i \nu_{ie} (\boldsymbol{v}_i - \boldsymbol{v}_e) - m_i n_i \nu_{in} \boldsymbol{v}_i, \tag{A.1 c}$$
$$\nabla \cdot \boldsymbol{J} = 0. \tag{A.1 d}$$

Here, n_e is the electron density, $\boldsymbol{J}$ is the electric current, and $m_j, \boldsymbol{v}_j$ and p_j are the mass, the velocity and the pressure of the jth species, respectively, where j corresponds to the electron(e) and ion(i). The magnetic field is given as $\boldsymbol{B} = B\boldsymbol{b}$ ($\boldsymbol{b}$ is the unit vector directed to the magnetic field), and ϕ is the electrostatic potential. The collision frequencies between electron and ion, ion and electron, ion and neutrals are denoted by ν_{ei}, ν_{ie} and ν_{in}, respectively. Noted that in order to guarantee the momentum conservation between the electron and ion, $m_e\nu_{ei} = n_i\nu_{ie}$ holds. Then we normalize the variables as

$$\omega_{ci} t \to t, \qquad \rho_s \nabla \to \nabla, \qquad \boldsymbol{v}_j / c_s \to \boldsymbol{v}_j, \qquad \nu_j / \omega_{ci} \to \nu_j,$$
$$e\phi / T_e \to \phi, \qquad \ln (n_e / n_0) \to N,$$

where n_0 is the constant value for the electron density. The ion gyro-frequency and gyro-radius are ω_{ci} and $\rho_s = \omega_{ci}^{-1} c_s$, respectively, and the sound speed, c_s, is given by $\sqrt{T_e/m_i}$. Then, Eqs. (A.1 a)-(A.1 c) are rewritten as

$$\partial_t N + \boldsymbol{v}_e \cdot \nabla N + \nabla \cdot \boldsymbol{v}_e = 0, \tag{A.2 a}$$
$$d_t \boldsymbol{v}_e = \frac{m_i}{m_e} (-\nabla N + \nabla\phi - \boldsymbol{v}_e \times \boldsymbol{b}) - \nu_{ei} (\boldsymbol{v}_e - \boldsymbol{v}_i), \tag{A.2 b}$$
$$d_t \boldsymbol{v}_i = -\frac{T_i}{T_e} \nabla N - \nabla\phi + \boldsymbol{v}_i \times \boldsymbol{b} - \nu_{in} \boldsymbol{v}_i - \nu_{ie} (\boldsymbol{v}_i - \boldsymbol{v}_e). \tag{A.2 c}$$

In the derivation of the above equations, we use the assumption that both the electron and ion temperatures are spatially homogeneous. In the following, we assume the cold ion $T_i/T_e \ll 1$, and neglect the first term of Eq. (A.2 c). From Eqs. (A.2 b) and (A.2 c), neglecting the inertial term (polarization drift) for electron, the drift motions for the electron and ion are derived as

$$\boldsymbol{v}_e = \boldsymbol{b} \times \nabla (\phi - N) + v_{e,\parallel} \boldsymbol{b}, \tag{A.3 a}$$
$$\boldsymbol{v}_i = \boldsymbol{b} \times \nabla\phi - d_t \nabla_\perp \phi - \nu_{in} \nabla_\perp \phi + v_{i,\parallel} \boldsymbol{b}. \tag{A.3 b}$$

Using the parallel component of the equation of motion for electron without the inertia term, the relative parallel velocity is given as

$$v_{e,\parallel} - v_{i,\parallel} = D \nabla_\parallel (\phi - N), \tag{A.4}$$

where D is defined by $D = \nu_{ei}^{-1} m_i/m_e$. By using the charge neutrality condition, Eq. (A.1 d), and combining Eqs. (A.3 a), (A.3 b) and (A.4), the vorticity equation is obtained as

$$d_t \nabla_\perp^2 \phi + \nabla N \cdot d_t \nabla_\perp \phi = \\ -D\nabla_\parallel^2 (\phi - N) - D\nabla_\parallel N \nabla_\parallel (\phi - N) - \nu_{in} \left(\nabla_\perp^2 \phi + \nabla N \cdot \nabla_\perp \phi \right), \quad \text{(A.5)}$$

where the time derivative d_t is given as

$$d_t = \partial_t + \boldsymbol{b} \times \nabla\phi \cdot \nabla + v_{i,\parallel} \nabla_\parallel. \quad \text{(A.6)}$$

The ion parallel flow equation is obtained from Eq. (A.2 c) with Eq. (A.4) as

$$\begin{aligned} d_t v_{i,\parallel} &= -\nabla_\parallel \phi - \nu_{ie} \left(v_{e,\parallel} - v_{i,\parallel} \right) - \nu_{in} v_{i,\parallel}, \\ &= -\nabla_\parallel N - \nu_{in} v_{i,\parallel}, \end{aligned} \quad \text{(A.7)}$$

where $\nu_{ie} \left(v_{e,\parallel} - v_{i,\parallel} \right) = -\nabla_\parallel (\phi - N)$ is used (noted that $\nu_{ie} D = 1$). The continuity equation is obtained from Eq. (A.2 a) by substituting the velocity by the drift motion Eq. (A.3 a) as

$$\partial_t N + \boldsymbol{b} \times \nabla\phi \cdot \nabla N + v_{i,\parallel} \nabla_\parallel N + \nabla_\parallel v_{i,\parallel} = -D\nabla_\parallel^2 (\phi - N) - D\nabla_\parallel N \nabla_\parallel (\phi - N). \quad \text{(A.8)}$$

In this way, the complete set of the model equation, Eqs. (A.5), (A.7) and (A.8), is derived, which can describe the low frequency turbulence.

In this study, we further simplify the model. First, the turbulence wavelength in the parallel direction is assumed to be much longer than the perpendicular wavelength, $k_\parallel \ll k_\perp$, and the parallel nonlinearity term $D\nabla_\parallel N \nabla_\parallel (\phi - N)$ is neglected. Second, the terms in vorticity equation Eq. (A.5) which couple with the density and potential are neglected. Because these terms are much smaller than the others as

$$\left| \frac{-\nabla N \cdot d_t \nabla_\perp \phi}{\partial_t \nabla_\perp^2 \phi} \right| \sim \frac{1}{k_\perp L_n}, \\ \left| \frac{\nu \nabla N \cdot \nabla_\perp \phi}{\nu \nabla_\perp^2 \phi} \right| \sim \frac{1}{k_\perp L_n},$$

where L_n is the density scale length. The density scale length is usually much longer than the turbulence wavelength, so $k_\perp L_n \gg 1$ is satisfied. Under this situation, the model equation is obtained as in Eqs. (1a)-(1c).

References

[1] K. Ida. Experimental studies of the physical mechanism determining the radial electric field and its radial structure in a toroidal plasma. *Plasma Physics and Controlled Fusion*, 40(8):1429, 1998.

[2] Ö. D. Gürcan, P. H. Diamond, T. S. Hahm, and R. Singh. Intrinsic rotation and electric field shear. *Physics of Plasmas*, 14(4):042306, 2007.

[3] J. E. Rice, J. W. Hughes, P. H. Diamond, Y. Kosuga, Y. A. Podpaly, M. L. Reinke, M. J. Greenwald, Ö. D. Gürcan, T. S. Hahm, A. E. Hubbard, et al. Edge temperature gradient as intrinsic rotation drive in alcator c-mod tokamak plasmas. *Physical review letters*, 106(21):215001, 2011.

[4] P. H. Diamond, Y. Kosuga, Ö. D. Gürcan, C. J. McDevitt, T. S. Hahm, N. Fedorczak, J. E. Rice, W. X. Wang, S. Ku, J. M. Kwon, et al. An overview of intrinsic torque and momentum transport bifurcations in toroidal plasmas. *Nuclear Fusion*, 53(10):104019, 2013.

[5] N. D'Angelo. Kelvin—helmholtz instability in a fully ionized plasma in a magnetic field. *The Physics of Fluids*, 8(9):1748–1750, 1965.

[6] W. Horton, T. Tajima, and T. Kamimura. Kelvin–helmholtz instability and vortices in magnetized plasma. *The Physics of fluids*, 30(11):3485–3495, 1987.

[7] M. Sasaki, Y. Camenen, A. Escarguel, S. Inagaki, N. Kasuya, K. Itoh, and T. Kobayashi. Formation of spiral structures of turbulence driven by a strong rotation in magnetically cylindrical plasmas. *Physics of Plasmas*, 26(4):042305, 2019.

[8] T. Kaneko, H. Tsunoyama, and R. Hatakeyama. Drift-wave instability excited by field-aligned ion flow velocity shear in the absence of electron current. *Physical review letters*, 90(12):125001, 2003.

[9] P. J. Catto, M. N. Rosenbluth, and C. S. Liu. Parallel velocity shear instabilities in an inhomogeneous plasma with a sheared magnetic field. *The Physics of Fluids*, 16(10):1719–1729, 1973.

[10] X. Garbet, Y. Sarazin, P. h. Ghendrih, S. Benkadda, P. Beyer, C. Figarella, and I. Voitsekhovitch. Turbulence simulations of transport barriers with toroidal velocity. *Physics of Plasmas*, 9(9):3893–3905, 2002.

[11] S. S. Kim, H. Jhang, P. H. Diamond, L. Terzolo, S. Yi, and T. S. Hahm. Intrinsic rotation, hysteresis and back transition in reversed shear internal transport barriers. *Nuclear Fusion*, 51(7):073021, 2011.

[12] X. Garbet, C. Fenzi, H. Capes, P. Devynck, and G. Antar. Kelvin–helmholtz instabilities in tokamak edge plasmas. *Physics of Plasmas*, 6(10):3955–3965, 1999.

[13] Y. Kosuga, S.-I. Itoh, and K. Itoh. Density peaking by parallel flow shear driven instability. *Plasma and Fusion Research*, 10:3401024–3401024, 2015.

[14] S. Inagaki, T. Kobayashi, Y. Kosuga, S.-I. Itoh, T. Mitsuzono, Y. Nagashima, H. Arakawa, T. Yamada, Y. Miwa, N. Kasuya, M. Sasaki, et al. A concept of cross-ferroic plasma turbulence. *Scientific reports*, 6:22189, 2016.

[15] T. Kobayashi, S. Inagaki, Y. Kosuga, M. Sasaki, Y. Nagashima, T. Yamada, H. Arakawa, N. Kasuya, A. Fujisawa, S.-I. Itoh, et al. Structure formation in parallel ion flow and density profiles by cross-ferroic turbulent transport in linear magnetized plasma. *Physics of Plasmas*, 23(10):102311, 2016.

[16] M. Sasaki, K. Itoh, Y. Kosuga, J. Q. Dong, S. Inagaki, T. Kobayashi, J. Cheng, K. J. Zhao, and S.-I. Itoh. Parallel flow driven instability due to toroidal return flow in high-confinement mode plasmas. *Nuclear Fusion*, 59(6):066039, 2019.

[17] J. Cheng, J. Q. Dong, K. Itoh, S.-I. Itoh, L. W. Yan, J. Q. Xu, M. Jiang, Z. H. Huang, K. J. Zhao, Z. B. Shi, et al. Formation of radially elongated flow leading to onset of type-iii edge localized modes in toroidal plasmas. *Nuclear Fusion*, 60(4):046021, 2020.

[18] S. Oldenbürger, K. Uriu, T. Kobayashi, S. Inagaki, M. Sasaki, Y. Nagashima, T. Yamada, A. Fujisawa, S.-I. Itoh, and K. Itoh. Configuration of flows in a cylindrical plasma device. *Plasma and Fusion Research*, 7:2401146–2401146, 2012.

[19] N. Asakura, S. Sakurai, K. Itami, O. Naito, H. Takenaga, S. Higashijima, Y. Koide, Y. Sakamoto, H. Kubo, and G. D. Porter. Plasma flow measurement in high-and low-field-side sol and influence on the divertor plasma in jt-60u. *Journal of nuclear materials*, 313:820–827, 2003.

[20] M. Sasaki, N. Kasuya, K. Itoh, S. Toda, T. Yamada, Y. Kosuga, Y. Nagashima, T. Kobayashi, H. Arakawa, K. Yamasaki, et al. Topological bifurcation of helical flows in magnetized plasmas with density gradient and parallel flow shear. *Physics of Plasmas*, 24(11):112103, 2017.

[21] M. Sasaki, N. Kasuya, S. Toda, T. Yamada, Y. Kosuga, H. Arakawa, T. Kobayashi, S. Inagaki, A. Fujisawa, Y. Nagashima, et al. Multiple-instabilities in magnetized plasmas with density gradient and velocity shears. *Plasma and Fusion Research*, 12:1401042–1401042, 2017.

[22] R. Hong, J. C. Li, R. Hajjar, T. S. Chakraborty, P. H. Diamond, and G. R. Tynan. Generation of parasitic axial flow by drift wave turbulence with broken symmetry: Theory and experiment. *Physics of Plasmas*, 25(5):055710, 2018.

[23] D. A. Schaffner, T. A. Carter, G. D. Rossi, D. S. Guice, J. E. Maggs, S. Vincena, and B. Friedman. Turbulence and transport suppression scaling with flow shear on the large plasma device. *Physics of Plasmas*, 20(5):055907, 2013.

[24] Y. Kosuga, M. Sasaki, and Z. B. Guo. Flow helicity of wavy plasma turbulence. *Physics of Plasmas*, 27(2):022303, 2020.

[25] N. Dupertuis, S. Inagaki, Y. Nagashima, Y. Kosuga, F. Kin, T. Kobayashi, N. Kasuya, M. Sasaki, A. Fujisawa, M. Q. Tran, et al. Coexistence of drift waves and d'angelo modes at different position and frequency in linear plasma device. *Plasma and Fusion Research*, 12:1201008–1201008, 2017.

[26] P. Vaezi, C. Holland, S. C. Thakur, and G. R. Tynan. Validation study of a drift-wave turbulence model for csdx linear plasma device. *Physics of Plasmas*, 24(9):092310, 2017.

[27] T. Windisch, O. Grulke, and T. Klinger. Radial propagation of structures in drift wave turbulence. *Physics of Plasmas*, 13(12):122303, 2006.

[28] Y. Saitou, A. Yonesu, S. Shinohara, M. V. Ignatenko, N. Kasuya, M. Kawaguchi, K. Terasaka, T. Nishijima, Y. Nagashima, Y. Kawai, et al. Reduction effect of neutral density on the excitation of turbulent drift waves in a linear magnetized plasma with flow. *Physics of plasmas*, 14(7):072301, 2007.

[29] N. Kasuya, S. Abe, M. Sasaki, S. Inagaki, T. Kobayashi, and M. Yagi. Turbulence simulation taking account of inhomogeneity of neutral density in linear devices. *Physics of Plasmas*, 25(1):012314, 2018.

[30] T. Kobayashi, F. Kin, Y. Kawachi, M. Sasaki, Y. Kosuga, K. Yamasaki, and S. Inagaki. Impact of helium neutral gas puff on plasma turbulence in linear magnetized argon plasmas. *Physics of Plasmas*, submitted (2020).

[31] BN Rogers and Paolo Ricci. Low-frequency turbulence in a linear magnetized plasma. *Physical review letters*, 104(22):225002, 2010.

[32] Dustin M Fisher, Barrett N Rogers, Giovanni D Rossi, Daniel S Guice, and Troy A Carter. Three-dimensional two-fluid braginskii simulations of the large plasma device. *Physics of Plasmas*, 22(9):092121, 2015.